Supplementary Materials for

Regulation and targeting of androgen receptor nuclear localization in castration-resistant prostate cancer

Supplementary Figure legends

Supplementary Figure 1. (A) Western blot analysis of indicated AR constructions in COS-7 cells. **(B-F)** The quantification results of Fig. 1B-F. The GFP fluorescence of each indicated constructs in the cytoplasm and nucleus was quantitated using Image J software (n = 6). **(G)** Represented fluorescent images of GFP 24 hours after treatment with DMSO, MG132 or DHT in presence of CHX (Cycloheximide). **(H)** Representative fluorescent images of transfected GFP-NES^{PKI} in COS-7 cells treated DMSO or MG132 in presence or absence of CHX. Quantitative data are presented as the mean ± SD and all the data represent 1 of 2 independent experiments with consistent results. Unpaired t-test (**B-F**) was used to determine statistical significance. ***$P < 0.001$.

Supplementary Figure 2. Imported nuclear AR is degraded and not exported following DHT withdrawal. (A) The quantification results of Fig. 2A. The GFP-AR fluorescence in cytoplasm and nucleus was quantitated using Image J software (n = 6). **(B)** Representative fluorescent images of endogenous AR in LNCaP cells treated with DHT followed by DHT withdrawal (W/D) and CHX in presence or absence of MG132 (n = 6). **(C)** Western blot analysis of nuclear and cytoplasmic extracts of endogenous AR in C4-2 cells after DHT withdrawal in presence or absence of MG132. **(D)** Representative fluorescent images of GFP-AR or ReAsH pulse labeled GFP-AR-4Cys. **(E-F)** The quantification results of Fig. 2C. The ReAsH fluorescence in cytoplasm and nucleus was quantitated using Image J software (n = 6). Quantitative data are presented as the mean ± SD and all the data represent 1 of at least 2 independent experiments with consistent results. Unpaired t-test (**A,** COS-7 & **B,** W/D versus DHT) or Mann-Whitney test (**A,** LNCaP & **F,** W/D versus DHT) was used to determine statistical significance. **$P < 0.01$, ***$P < 0.001$.

Supplementary Figure 3. Unliganded AR can be imported into the nucleus in presence of MG132. (A) The quantification results of Fig. 3A. The GFP-AR fluorescence in cytoplasm

and nucleus was quantitated using Image J software (n = 6). **(B)** Schematic of pulse-chase experiments using ReAsH. **(C)** Representative fluorescent images of ReAsH pulse-chase assay. GFP-AR-4Cys was transfected into COS-7, LNCaP and C4-2 cells for 24 hours in CSS medium and labelled by ReAsH. Then the images were captured at 24 hours after MG132 or DHT treatment. Total GFP-AR-4Cys was *green* signal. The ReAsH labelled protein was as *red* signal. The ReAsH fluorescence in cytoplasm and nucleus was quantitated using Image J software (n = 6). **(D)** The quantification results of Fig. 3C. The GFP fluorescence in cytoplasm and nucleus was quantitated using Image J software (n = 6). Quantitative data are presented as the mean ± SD and all the data represent 1 of at least 2 independent experiments with consistent results. One-way ANOVA with Dunnett's multiple-comparisons post-test (**A, C, & D**) was used to determine statistical significance. $*P < 0.05$, $**P < 0.01$, $***P < 0.001$.

Supplementary Figure 4. AR nuclear import rate was similar between the HSPC LNCaP and CRPC C4-2 cells. (A) C4-2 cells stably transfected with GFP-AR-GFP were pre-treated with CPPI for 24 hours in CSS medium. Then the GFP-AR-GFP images were captured at indicated time points after CPPI withdrawal, in the presence of CHX plus increasing doses of DHT. **(B-C)** Representative fluorescent images of ReAsH pulse-chase assay. The GFP-AR-4Cys expression vector was transfected into COS-7, LNCaP and C4-2 cells and then pre-treated with CPPI for 24 hours in CSS medium. The transfected AR was labelled by ReAsH and the intensity of labelled AR was detected at different time in the absence or presence of MG132 in CSS medium **(B)** or in the presence of 0.01n M DHT (**C**)**.** GFP-AR was *green* signal. The ReAsH labelled protein was as *red* signal. The ReAsH fluorescence in the nucleus was quantitated using Image J software (n = 6). Quantitative data are presented as the mean ± SD and all the data represent 1 of 2 independent experiments with consistent results.

Supplementary Figure 5. AR is polyubiquitinated in the nuclei and regulated by MDM2 and PP1α. (A) C4-2 cells were transfected with MDM2 siRNA. The expression levels of nuclear and cytoplasmic AR were detected through Western blot. **(B)** Western blot analysis of ubiquitin (Ub) and AR in C4-2 cells in the presence of MG132. **(C)** Expression of transfected YFP-PP1α in LNCaP cells. **(D-E)** Western blot analysis of ubiquitin (Ub) and AR in wild-

type AR transfected HEK 293 cells **(D)** and LNCaP cells **(E)** in presence of MG132. Data represent 1 of 2 independent experiments with consistent results.

Supplementary Figure 6. (A) Representative images of TUNEL staining on C4-2 xenografts treated with CPPI (n=5). **(B)** Patient-derived explants were treated with CPPI. Effect of CPPI on AR expression with representative sections are shown (n = 3). Data are presented as the mean ± SD. Unpaired t-test (**B**) was used to determine statistical significance. $^{**}P < 0.01$.

Supplementary Figure 7. CPPI increased nuclear AR degradation and blocked AR nuclear import. (A) The quantification results of Fig. 5D. The ReAsH fluorescence in cytoplasm and nucleus was quantitated using Image J software (n = 6). **(B)** Western blot analysis of ubiquitin (Ub) and AR in LNCaP cells treated with or without CPPI for 24 hours in the presence of MG132. **(C)** Western blot analysis of Ub and Flag in Flag AR transfected HEK 293 cells treated with or without CPPI for 24 hours in the presence of MG132. The IP samples were also analyzed by Western blot with additional indicated antibodies. **(D)** Time course of GFP-AR localization in transfected COS-7 cells treated with DMSO, 30 μM CPPI or 10 μM Enzalutamide in the presence of MG132 in CSS medium. The nuclear GFP-AR quantification data are shown at right. **(E)** Time course of GFP-AR localization in transfected COS-7 cells treated with DMSO or 30 μM CPPI in the presence of MG132 and/or 1 nM DHT. The nuclear GFP-AR quantification data are shown at right. **(F)** Cell cycle analysis of LNCaP and C4-2 cells treated with CPPI (n = 3). **(G)** PC3 and HEK 293 Cells were transiently transfected with GFP-AR^{WT}, pPSA6.1-Luc, and pRL-TK. The cells were treated with R1881 with or without CPPI. Firefly luciferase values were determined and normalized to Renilla (n = 3). Quantitative data are presented as the mean ± SD and all the data represent 1 of at least 2 independent experiments with consistent results. One-way ANOVA with Dunnett's multiple-comparisons post-test (**F & G**) was used to determine statistical significance. $^{**}P < 0.01$, $^{***}P < 0.001$.

Supplementary Figure 8. CPPI is an AR competitive inhibitor. (A) $ITDRF_{CETSA}$ experiments performed for DHT in the presence of 10 μM MG132 in C4-2 cells (n = 1). **(B)** Western blot analysis of protein levels of AR in C4-2 cells treated with indicated CPPI for 90

minutes in 37 °C. **(C)** COS-7 transfected COS-7 cells were incubated with 1 nM [^{3}H] DHT and the indicated amount of CPPI. The retained [^{3}H] DHT in COS-7 cells were counted (n = 1). **(D)** The output of the PyRx™ computational model using the AutoDock Vina™ docking algorithm.

Supplemental Figure S9. (A) Representative fluorescent images of GFP-ARv7 transfected COS-7 cells after 48 hours treatment with CPPI. Lower panel shows the quantification of nuclear GFP-ARv7 intensity (n = 6). **(B)** Representative images of BrdU staining in ARv7 stable expression PC-3 cells treated with CPPI. Lower panel shows percentages of the PC-3 cells stained with BrdU (n = 3). **(C)** BRET assay of AR-FL and Arv7 in transfected into HEK 293 cells. Left panel: Western blotting with a pan-AR antibody; Right panel: BRET saturation curves of AR-FL and ARv7 at different ratios (n = 3). Data are presented as the mean ± SD and represent 1 of 2 independent experiments with consistent results.

Supplementary Figure 1

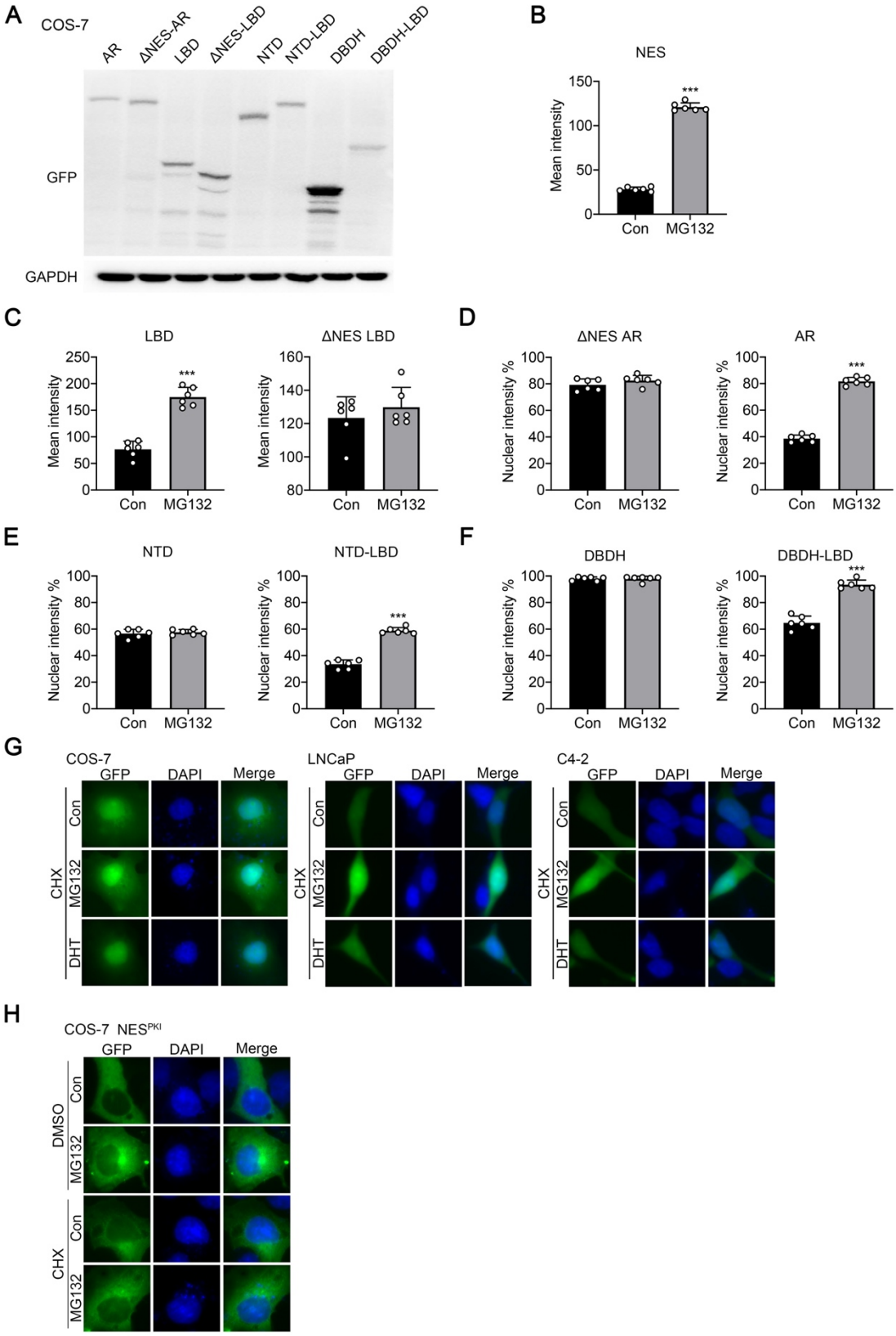

Supplementary Figure 2

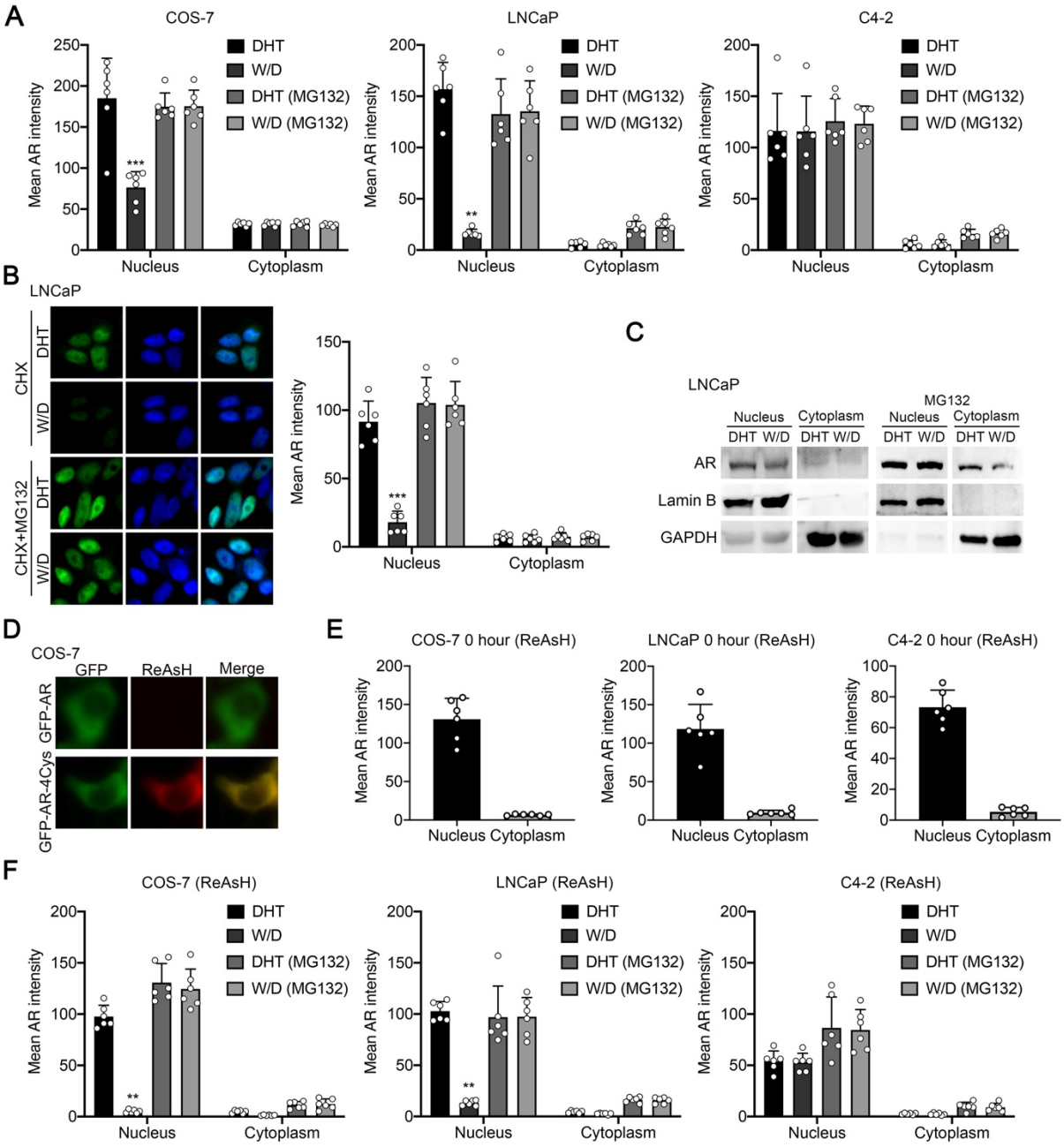

Supplementary Figure 3

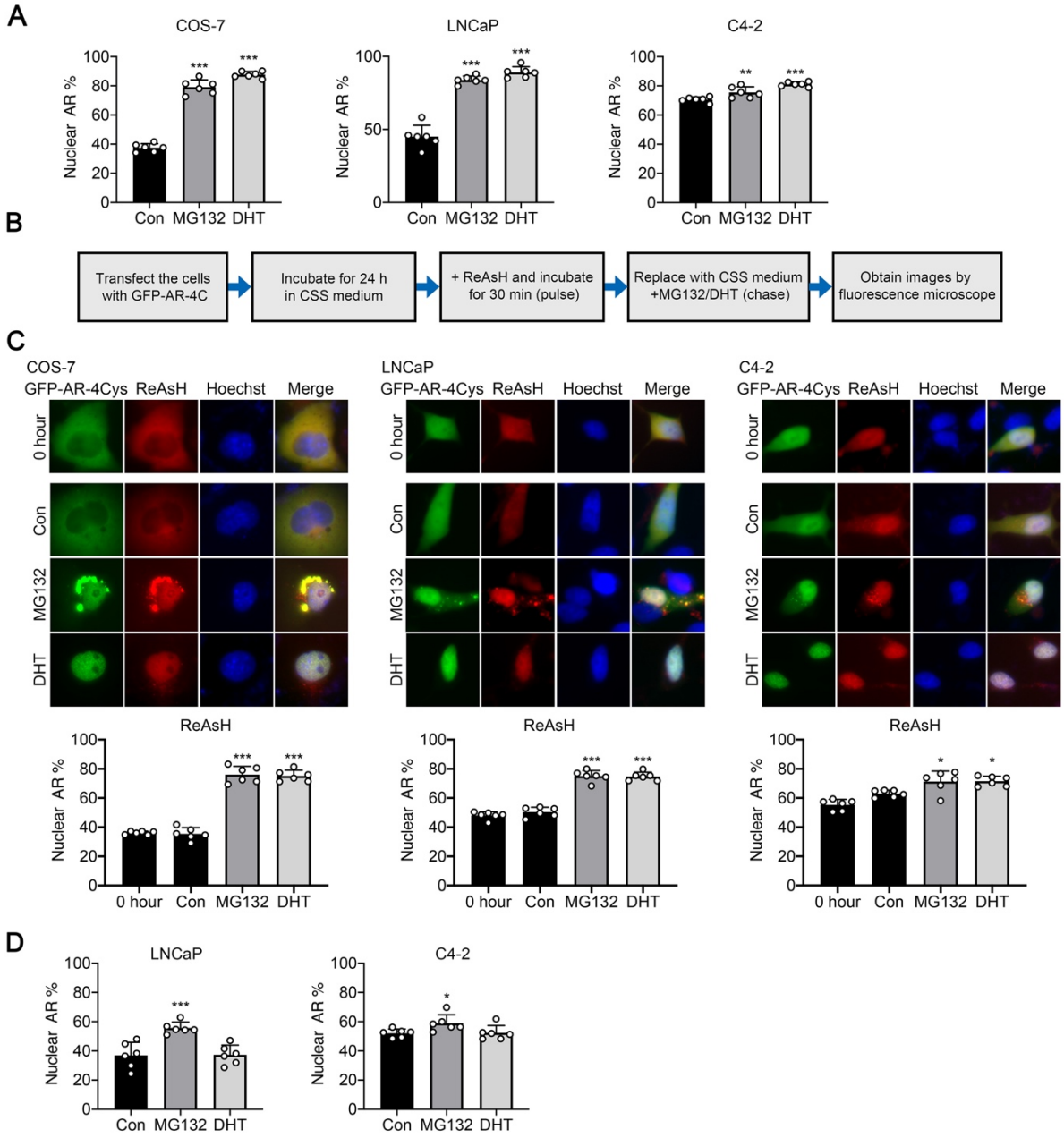

Supplementary Figure 4

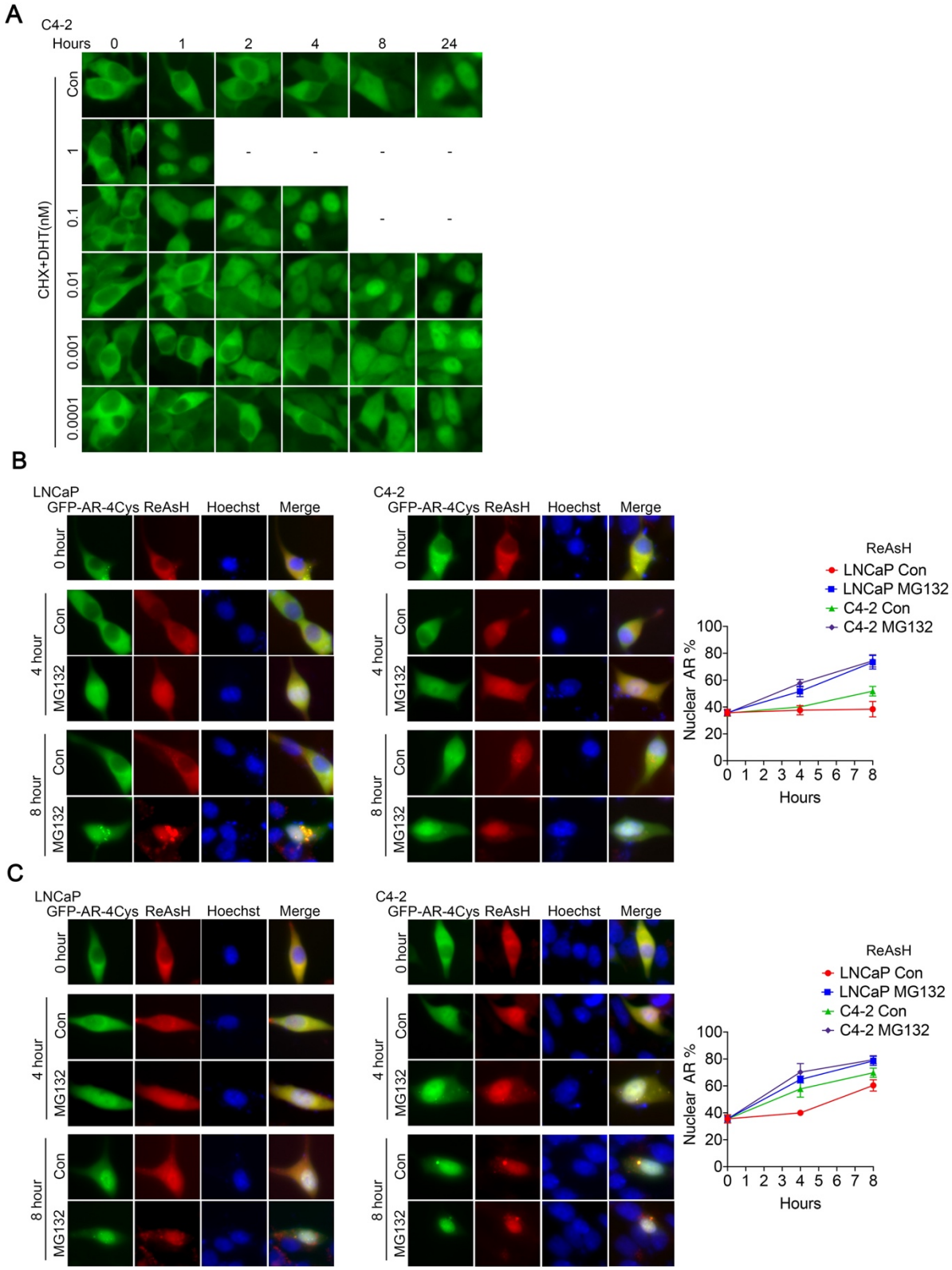

Supplementary Figure 5

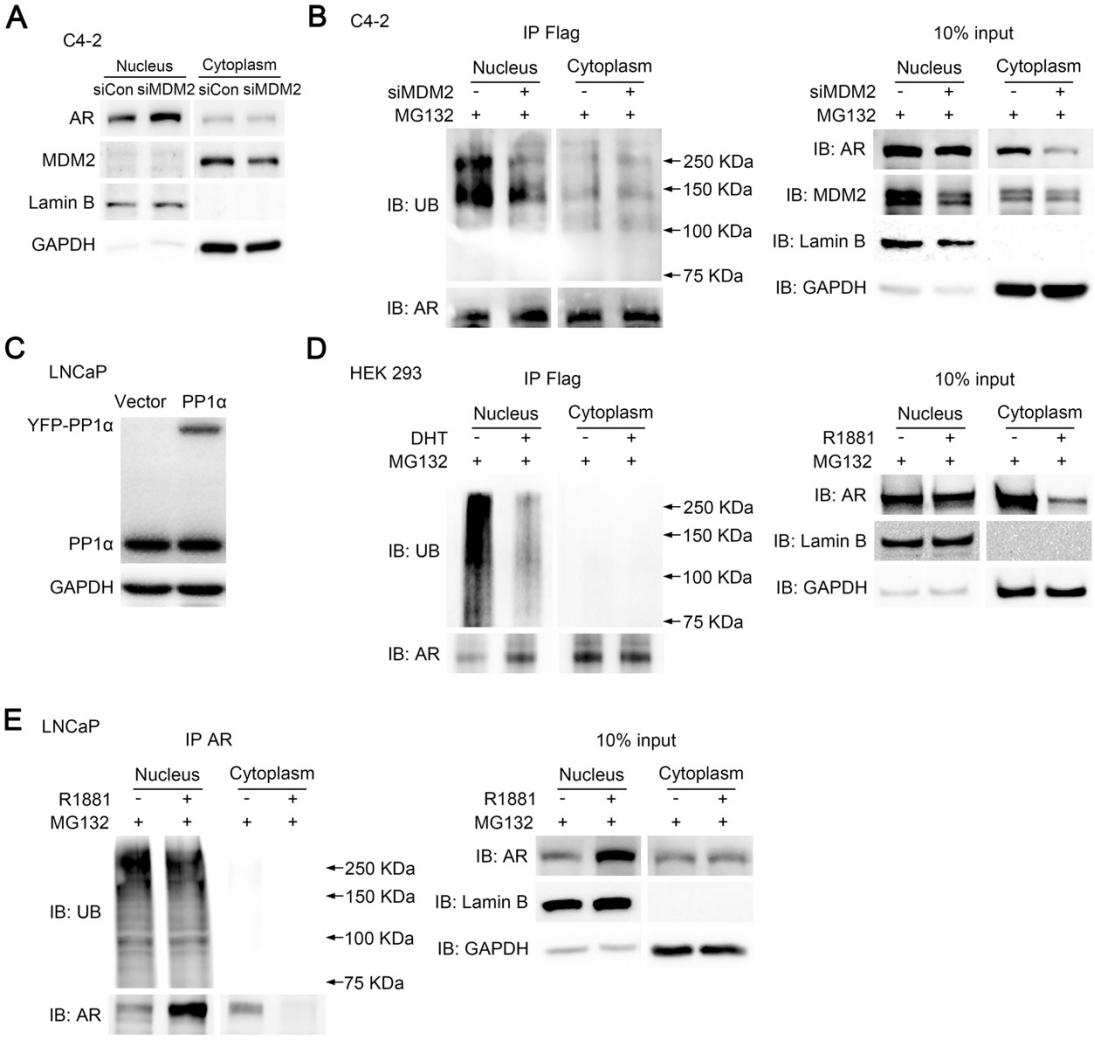

Supplementary Figure 6

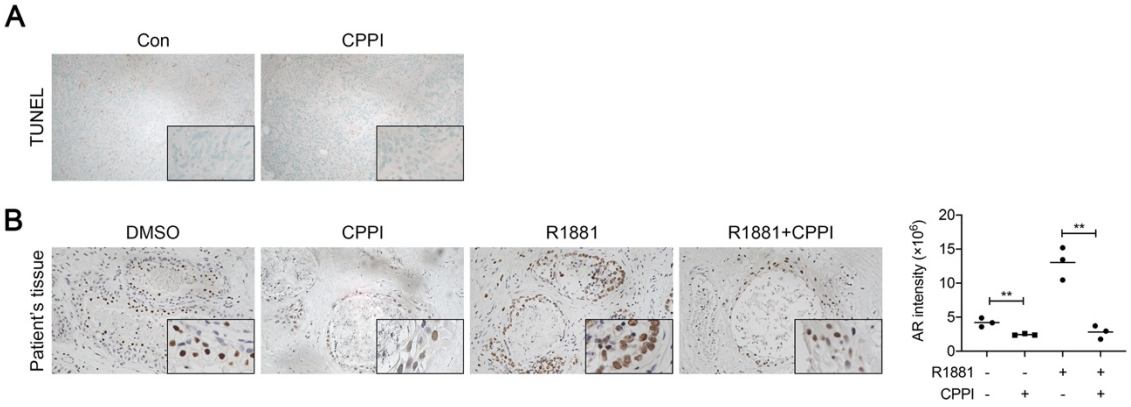

Supplementary Figure 7

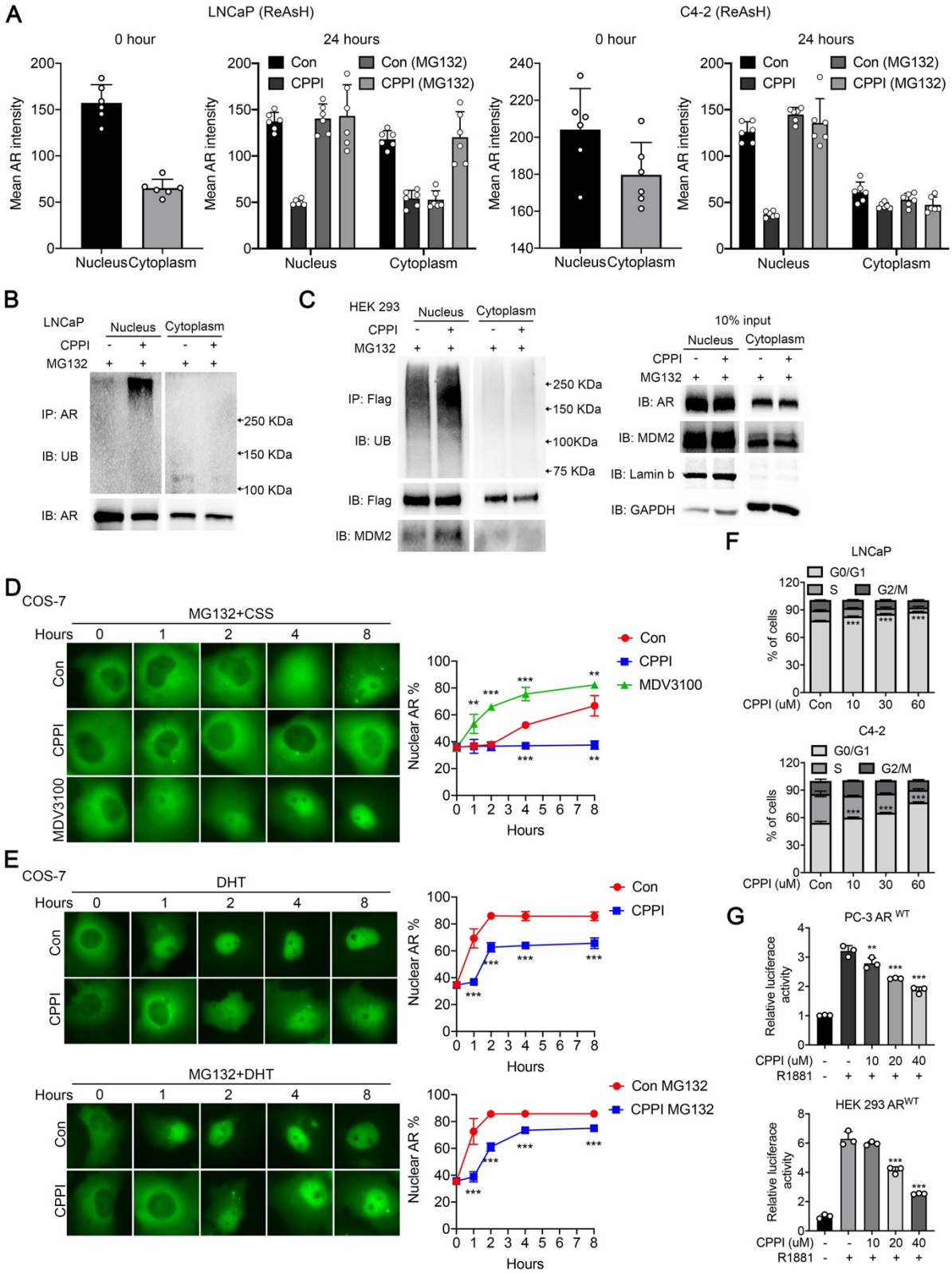

Supplementary Figure 8

A

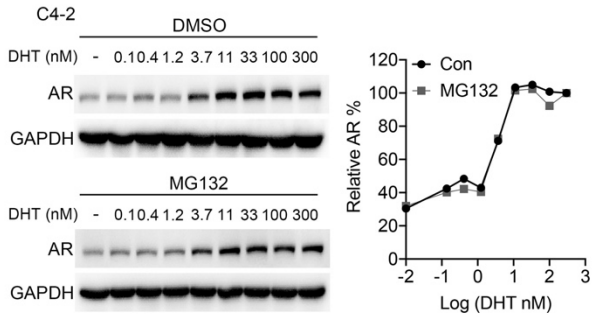

B

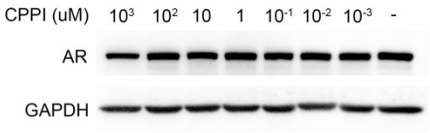

C

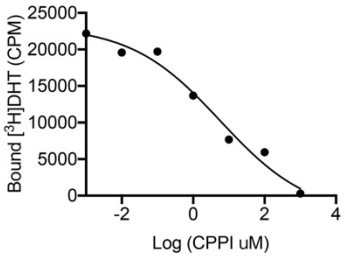

D

Ligand	Binding Affinity (kcal/mol)	rmsd/ub	rmsd/lb
lbd_DHT_uff_E=438.03	-11.3	0	0
lbd_14742211_uff_E=397.46	-7.5	0	0
lbd_14742211_uff_E=397.46	-7.4	5.617	3.271
lbd_14742211_uff_E=397.46	-7.3	12.119	10.851
lbd_14742211_uff_E=397.46	-6.8	13.549	12.176
lbd_14742211_uff_E=397.46	-6.4	12.704	11.392
lbd_14742211_uff_E=397.46	-6.1	14.279	11.927
lbd_14742211_uff_E=397.46	-5.8	15.931	14.812
lbd_14742211_uff_E=397.46	-5.6	15.656	13.661
lbd_14742211_uff_E=397.46	-5.6	24.163	23.356

Supplementary Figure 9

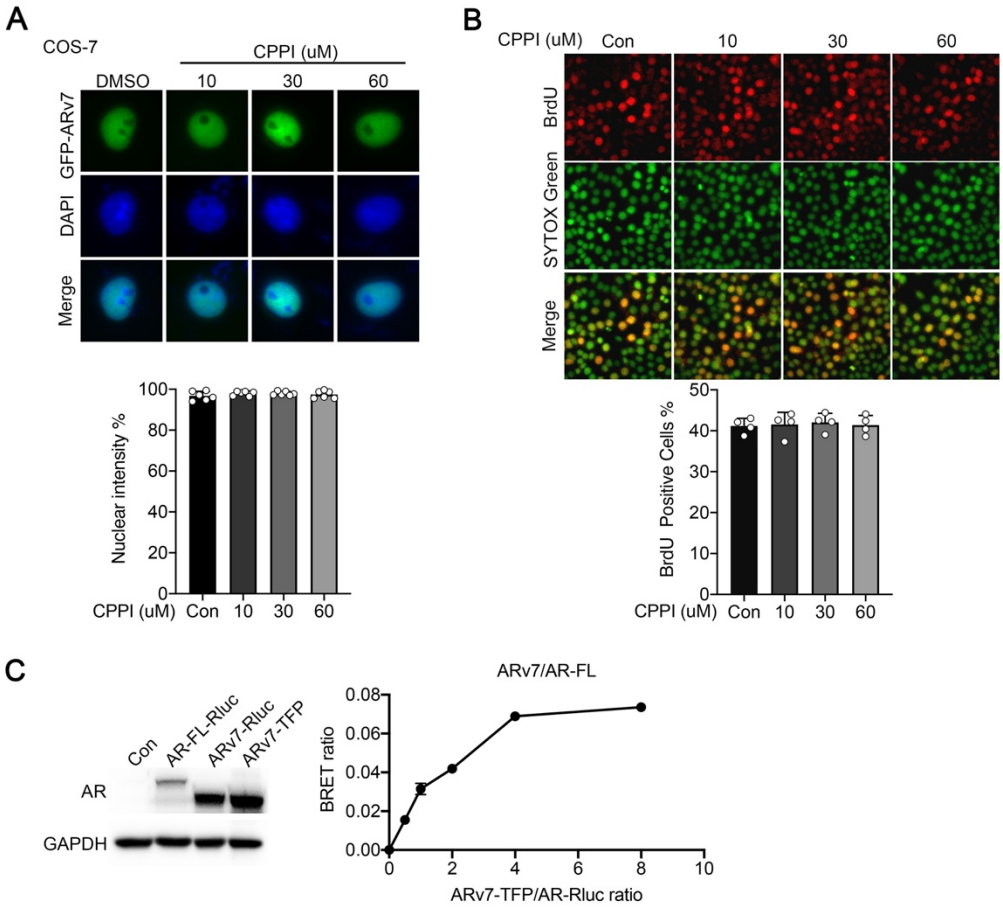

Supplemental Table 1. Primer sequence used in qRT-PCR analysis

Name	Forward Primer	Reverse Primer
KLK3	CAGGTGTAGACCAGAGTGTTTC	CTGTGTCCTCAGAGAAATTGAGT
TMPRSS2	TGCTCCAACTCTGGGATAGA	GGATGAAGTTTGGTCCGTAGAG
NKX3-1	TCTGACAGGTGAATTGGATGG	GATTGGAGCAGGGTTTGTTATG
UBE2C	AAAGTGGTCTGCCCTGTATG	GGGACTATCAATGTTGGGTTCT
CDC20	AAGACCTGCCGTTACATTCC	ACATTCCCAGAACTCCAATCC
GAPDH	CTCCTCACAGTTGCCATGTA	GTTGAGCACAGGGTACTTTATTG